Global Change Biology (1999) **5,** 891–902

Seasonal patterns and environmental control of carbon dioxide and water vapour exchange in an ecotonal boreal forest

D. Y. HOLLINGER,*† S. M. GOLTZ,‡ E. A. DAVIDSON,§ J. T. LEE,‡ K. TU† and H. T. VALENTINE*

**USDA Forest Service, 271 Mast Rd., Durham, NH 03824, USA, †Department of Natural Resources, University of New Hampshire, Durham, NH 03824, USA, ‡Department of Applied Ecology and Environmental Sciences, University of Maine, Orono, ME 04469, USA, §Woods Hole Research Center, 13 Church St., Woods Hole, MA 02543, USA*

Abstract

Carbon dioxide, water vapour, and sensible heat fluxes were measured above and within a spruce dominated forest near the southern ecotone of the boreal forest in Maine, USA. Summer, mid-day carbon dioxide uptake was higher than at other boreal coniferous forests, averaging about $-13\,\mu mol\ CO_2\ m^{-2}\ s^{-1}$. Nocturnal summer ecosystem respiration averaged $\approx 6\,\mu mol\ CO_2\ m^{-2}\ s^{-1}$ at a mean temperature of $\approx 15\,^{\circ}C$. Significant ecosystem C uptake began with the thawing of the soil in early April and was abruptly reduced by the first autumn frost in early October. Half-hourly forest CO_2 exchange was regulated mostly by the incident photosynthetically active photon flux density (PPFD). In addition to the threshold effects of freezing temperatures, there were seasonal effects on the inferred photosynthetic parameters of the forest canopy. The functional response of this forest to environmental variation was similar to that of other spruce forests. In contrast to reports of carbon loss from northerly boreal forest sites, in 1996 the Howland forest was a strong carbon sink, storing about $2.1\,t\,C\,ha^{-1}$.

Keywords: AmeriFlux, Bowen ratio, carbon exchange, eddy covariance

Received 17 September 1998; resubmitted and accepted 9 February 1999

Introduction

Atmospheric studies based on flask samples of ambient air and models of atmospheric transport suggest that terrestrial ecosystems between 30°N and 65°N are major sinks for anthropogenically produced CO_2, removing from the atmosphere the equivalent of up to 40% of fossil fuel carbon emissions (Tans *et al*. 1990; Conway *et al*. 1994; Ciais *et al*. 1995). However, uptake in this latitudinal band can vary strongly on a short-term basis. For example, CO_2 uptake in the northern hemisphere above 30°N doubled between 1986 and 1992 (Conway *et al*. 1994) with most of this increase taking place on land (Ciais *et al*. 1995; Bender *et al*. 1996; Keeling *et al*. 1996). Between 1991 & 1992 alone, the northern terrestrial sink increased by almost 1 GT carbon.

More recently, researchers have used micrometeorological techniques to measure surface–atmosphere fluxes directly at several locations in the boreal zone (e.g. Fan *et al*. 1995; Baldocchi & Vogel 1996; Black *et al*. 1996; Baldocchi *et al*. 1997; Goulden *et al*. 1997, 1998; Jarvis *et al*. 1997; Hollinger *et al*. 1998). These studies indicate that boreal forests vary widely in their rate of CO_2 exchange. In a multiyear study, Goulden *et al*. (1998) found that the BOREAS northern spruce site (55.9°N, 98.5°W) has fluctuated between being a carbon source and sink since 1994.

This variability in both broad and local-scale measurements is surprising and of great potential concern as CO_2 and other greenhouse gas emissions continue to alter the climate. In order to predict future atmospheric CO_2 levels, we must quickly develop an understanding of how the climate system affects ecosystem processes which feedback to regulate atmospheric CO_2 levels.

We report here results for 1996 from an ongoing study of forest–atmosphere CO_2 exchange carried out near the southern ecotone of the boreal forest in eastern North

Correspondence: David Y. Hollinger, tel + 1/603-868-7673, fax + 1/603-868-7604, e-mail davidh@christa.unh.edu

America using the eddy covariance technique. Short-term environmental and seasonal regulation of CO_2 exchange in this evergreen coniferous forest are contrasted with similar processes operating in other forest types.

Methods

Site description

The Howland Forest AmeriFlux research site is located on land owned by the International Paper Timberlands Operating Company, Ltd. about 35 miles north of Bangor, ME, USA (45°12′ N, 68°44′ E, 60 m a.s.l.). The natural stands in this boreal–northern hardwood transitional forest are about 20 m tall and consist of spruce–hemlock–fir, aspen–birch, and hemlock–hardwood mixtures. The forest composition in a 3-ha plot 100 m from the tower was about 41% red spruce (*Picea rubens* Sarg.), 25% eastern hemlock (*Tsuga canadensis* (L.) Carr.), 23% other conifers (primarily balsam fir, *Abies balsamea* (L.) Mill., white pine, *Pinus strobus* L., and northern white cedar, *Thuja occidentalis* L.) and 11% hardwoods (red maple, *Acer rubrum* L. and paper birch, *Betula papyrifera* Marsh.) (Table 1). The live basal area of the plot was $32.2\,m^2\,ha^{-1}$. This forest was logged selectively around 1900, and under present commercial practices would have been recut about 1975. Compared to other commercial forests in the region, the stand is now considered 'overmature'.

The landscape around the site varies from flat to gently rolling, with a maximum elevation change of less than 68 m within 10 km. Due to the region's glacial history, soil drainage classes within a small area may vary widely, from well drained to poorly drained. Generally, the soils throughout the forest are glacial tills, acid in reaction, with low fertility and high organic composition. The climate is chiefly cold, humid, and continental and the region exhibits a snowpack of up to 2 m from December through March (Fernandez *et al*. 1993). Temperature and rainfall at the site in 1996 (6.2 °C and 1148 mm) were similar to the 1905–85 average values (calculated from Vose *et al*. 1992) at the nearby Orono station of 6.1 ± 1.0 °C and 988 ± 170 mm (mean and standard deviation).

The leaf area index (LAI) of the stand was not measured during the flux measurements reported here. In 1998, however, the stand LAI was measured on 6 different dates at 15 fixed locations to the north-west of the tower using two LiCor model LAI-2000 leaf area meters. A correction of 1.5 was applied to the leaf area meter data (Fassnacht *et al*. 1994; Stenberg 1996).

Measuring ecosystem carbon and water vapour exchange

Carbon dioxide, water vapour, heat, and momentum fluxes at a height of 29 m were measured from 1 January to 31 December 1996 by the eddy covariance technique (Baldocchi *et al*. 1988). Below-canopy fluxes were measured at 3 m from 22 May to 31 December 1996. The above- and below-canopy flux systems were based on model SAT-211/3K 3-axis sonic anemometers (Applied Technologies, Inc., Boulder, CO) and model LI-6262 fast response CO_2/H_2O infrared gas analysers (LiCor Inc., Lincoln, NB). These instruments were read at 5 Hz through RS-232 ports on two 386-class computers. The instruments and computers were protected from transients and voltage interruptions with surge suppressers and an uninterruptible power supply. Data were stored on internal hard drives and archived on CD-Rs. Air was ducted to the infrared gas analysers through ≈50 m of 3.2 mm diameter high-density polyethylene tubing at a mass flow rate of $4\,L\,min^{-1}$, regulated by mass flow controllers. Air pressures in the analysers were ≈80 KPa.

Ambient CO_2 concentrations at heights of 8.5, 13.5, 19.5, and 26.5 m were recorded with a system

Table 1 Tree density and basal area at the Howland flux measurement site

Species	Density (stems ha^{-1})	% of total living	Basal area ($m^2\,ha^{-1}$)	% of total living
Picea rubens	816	40.5	14.20	44.1
Tsuga canadensis	509	25.3	8.45	26.2
Hardwoods[1]	224	11.1	2.67	8.3
Thuja occidentalis	201	9.9	3.29	10.2
Abies balsamea	194	9.6	0.74	2.3
Pinus strobus	64	3.2	2.76	8.6
Total living	2017	100	32.2	100
Standing dead	585	–	4.7	–
Total	2602	–	36.9	–

[1]Primarily red maple, *Acer rubrum*, and paper birch, *Betula papyrifera*.

consisting of a LiCor nondispersive infrared gas analyser (Model 6251, LiCor, Inc., Lincoln, NB, USA), pumps, switching manifold, PTFE inlet tubes (i.d. = 4 mm) and data logger (Model 21X, Campbell Scientific Inc., Logan, UT, USA).

Flux calculations and corrections

Covariances were computed in real-time with a running-mean removal technique based on a digital recursive filter with a time constant of 600 s (McMillen 1988). This time constant was found to maximize the covariance between the vertical wind velocity and CO_2 concentration. Two-angle coordinate rotations were performed on the wind data in the covariance calculations to remove the effects of instrument tilt or terrain irregularity on the airflow. Variations in air density (e.g. Webb *et al*. 1980) were removed with copper heat exchangers in the air lines and via software based on simultaneous measurement of water vapour densities. Covariances between CO_2 and the vertical wind velocity (w) and between H_2O and w were calculated by digitally lagging the w signal to account for the transit time of the air sample down the inlet tube (McMillen 1988). Calculations were made for lags bracketing the expected lag (based on flow/volume calculations) over each 30 min, and the lag providing the maximum lag-covariance used in subsequent flux calculations. This approach fails when CO_2 or H_2O flux rates approach zero (evenings and early morning for CO_2, late night for H_2O) and lags from nearby suitable periods were used at these times. The timing of the maximum in the lagged covariances typically varied by < 6%.

The sensible heat flux (H, W m^{-2}) was calculated as

$$H = \frac{M_a C_p}{V} \cdot (\overline{w'T'} - (3.2 \cdot 10^{-4} \cdot T_K \cdot \overline{w'q'})), \qquad (1)$$

where M_a is the molecular weight of dry air (g mol^{-1}), C_p is the specific heat of dry air (J°K^{-1} g^{-1}), V is the molar volume of air at the ambient temperature and pressure (m^3 mol^{-1}), $\overline{w'T'}$ is the covariance between the vertical wind velocity and air temperature estimated from the sonic temperature (ms^{-1}°K^{-1}), $\overline{w'q'}$ is the covariance between the vertical wind velocity and the atmospheric water vapour concentration (ms^{-1} mol H_2O mol^{-1} air), and T_K is the actual air temperature estimated from the sonic temperature according to Kaimal & Gaynor (1991).

The latent heat flux (LE, W m^{-2}) was calculated as

$$LE = \lambda \frac{M_w \cdot \overline{w'q'}}{V}, \qquad (2)$$

where λ is the latent heat of vaporization (J g^{-1}), M_w is the molecular mass of water (g mol^{-1}), V is the molar volume of air (m^3 mol^{-1}), and $\overline{w'q'}$ is the covariance between the vertical wind velocity and atmospheric water vapour content (ms^{-1} mol H_2O mol^{-1} air).

The CO_2 eddy flux (F,μmol CO_2 m^{-2}s^{-1}) was calculated similarly

$$F = \frac{\overline{w'c'}}{V}, \qquad (3)$$

where $\overline{w'c'}$ is the covariance between the vertical wind and atmospheric carbon dioxide content (ms^{-1}μmol CO_2 mol^{-1} air) and V is as before.

Corrections for the spectral deficiencies of the system (tubing, analyser, and flow rate) were made following the procedure of Goulden *et al*. (1997). This involves the online calculation of an empirical transfer function rather than using formulations based on stability (e.g. Moore 1986). The measured, half-hourly carbon dioxide and water vapour fluxes are multiplied by H/H_f, where H_f is a sensible heat flux calculated with a temperature signal that has been digitally filtered to match the spectral response of the CO_2 and water vapour signals, respectively (Fig. 1a). For CO_2, these corrections averaged ≈ 6% during daytime hours and ≈ 11% at night (Fig. 1b). The water vapour time constant of our system was greater than that for CO_2, so the corrections to the H_2O flux were larger, averaging for our system ≈ 11% during the day and ≈ 19% at night. This approach does not yield stable correction values when $H \to 0$ (Fig. 1c) so fixed correction values of 20% for CO_2 and 32% for H_2O were used when $-15 < H < 10$ W m^{-2}. Since the CO_2 and H_2O fluxes were typically near zero at these times, errors in the spectral correction factors with small values of H were of little consequence. Goulden *et al*. (1997) found that the CO_2 flux underestimation (*loss*) increased linearly with wind during unstable and neutral periods as *loss* (%) = 1.9 + 1.67u, where u is the windspeed in ms^{-1}. For our system the relationship was; *loss* (%) = 2.8 + 0.7u, the differences presumably relating to physical differences between the flux systems and vegetation at the sites.

Flux values from both systems were excluded from further analysis if the wind speed was below 0.5 m s^{-1}, sensor variance was high (Hollinger *et al*. 1995), or rain or snow was falling. Data values were also excluded when the wind direction was 135 ± 1°; deficiencies in trigonometric functions in the software led to erroneous wind speeds under these conditions.

We measured three components of CO_2 exchange (μmol m^{-2}s^{-1}) between the forest ecosystem and the atmosphere; the turbulent eddy flux transported across the plane of instrumentation 29 m above the forest floor (F_e), an eddy flux at 3 m above the forest floor (F_f), and exchange below 29 m which is manifest as a change in the storage of CO_2 in the forest air column ($F_{\Delta S}$).

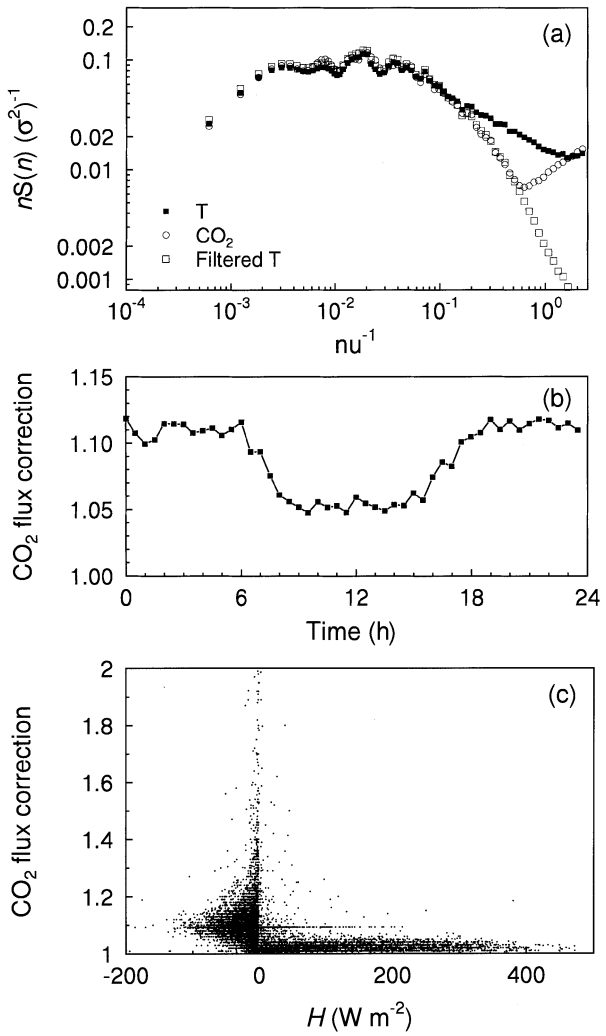

Fig. 1 (a) Average power spectra for temperature and CO_2 fluctuations over the Howland forest between 10.00 and 15.00 hours on 29 and 30 June 1996. Coefficients were found for a digital filter so that a filtered temperature response followed the CO_2 response. The upward trending values of the CO_2 spectra at normalized frequencies > 0.6 Hz is indicative of white noise and aliasing and does not affect the covariances. (b) Average CO_2 spectral corrections computed from the ratio of the unfiltered wT covariance to the wT covariance calculated with a temperature signal filtered to duplicate the response of the CO_2 analyser. (c) CO_2 flux correction as a function of the measured sensible heat flux.

We use a meteorological convention for our CO_2 measurements where carbon flux out of the ecosystem is defined as positive. The flux associated with a change in storage ($F_{\Delta S}$) is calculated by integrating the change in CO_2 concentration, c, through the air column as a function of height (z) up to the instrumentation plane (h):

$$F_{\Delta S} = \int_0^h \frac{dc}{dt} dz. \quad (4)$$

In the absence of advection, the daily net storage of CO_2 in the air column should be approximately zero. We integrated the half-hourly change in CO_2 concentration up to $h = 29$ m for our estimates of $F_{\Delta S}$. The net flux between the ecosystem and the atmosphere is the net ecosystem exchange (*NEE*). Over any time interval it is the sum of the eddy and storage fluxes:

$$NEE = F_e + F_{\Delta S}. \quad (5)$$

Over 24 h $F_{\Delta S} = 0$ so $NEE = F_e$. The net flux between the tree canopy and atmosphere (F_c) is the sum of the eddy and storage fluxes less the forest-floor flux (F_f):

$$F_c = F_e + F_{\Delta S} - F_f = NEE - F_f. \quad (6)$$

Ignoring $F_{\Delta S}$ will not affect 24-h flux estimates but may lead to under or over-estimates of assimilation at certain times of the day. In the early morning, for example, ignoring the contribution of $F_{\Delta S}$ to F_c would result in erroneously low values of F_c. This in turn could lead to errors in the inferred functional relationship between F_c and some environmental factor such as the photosynthetically active photon flux density (PPFD).

For our above canopy system, the nocturnal sum of F_e and $F_{\Delta S}$ was relatively constant when the friction velocity, u^* ($= \sqrt{\overline{w'u'}}$) ≥ 0.15 m s^{-1} (Fig. 2). However, when u^* was below this value, $F_e + F_{\Delta S}$ appeared to decline, suggesting an incomplete accounting of nocturnal CO_2 production, perhaps due to cold air draining down stream channels. For this work we adopted the approach of Jarvis *et al*. (1997) and omitted nocturnal flux values from further analysis when u^* was below a threshold, in this case of 0.15 m s^{-1}. We did not use the u^* threshold with our below canopy system; the requirement of a minimum half-hourly wind speed of 0.5 m s^{-1} resulted in the exclusion of data during calm periods.

Results

Energy exchange

The sum of sensible heat (H), latent heat (LE), soil heat flux (G), and canopy and forest air column heat storage (S) was close to the measured value of net radiation (R_n) for most half-hour time periods (Fig. 3). The slope of the best-fit regression ($H + LE + G + S = 1.03 * R_n - 28.7$, $r^2 = 0.90$) was similar to the expected value of 1, although the offset was unexpectedly high. A new net radiometer was installed in early 1997 and subsequent data suggests an offset closer to 0.

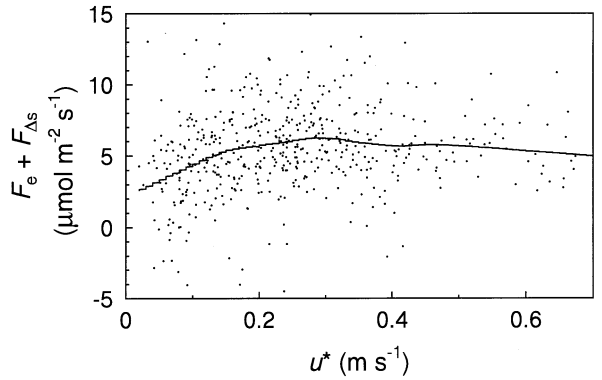

Fig. 2 The sum of the eddy and storage fluxes ($F_e + F_{\Delta S}$) during summer nights declines at low values of the momentum flux, u^*, indicating an incomplete accounting of nocturnal CO_2 production.

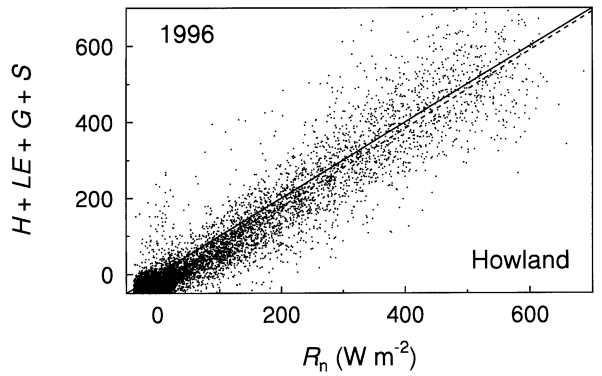

Fig. 3 Site energy balance for all data values in 1996. Latent energy was calculated based on the heat of sublimation for T_{air} < 0 °C. The slope of the linear regression (dashed line) was not significantly different from 1 (solid line).

The sensible heat flux from the Howland Forest increased from peak daily values of ≈200 W m^{-2} on sunny winter days to values of ≈400 W m^{-2} (Fig. 4) by early April (JD 90). Peak values of H were asymmetric with respect to the summer solstice, with higher values occurring prior to JD 170 rather than after this date. In contrast, winter values of LE were very low (< 50 W m^{-2}), and peak values remained low until air and soil temperatures exceeded freezing on about JD 100 (Fig. 4). Maximum values of LE approached 400 W m^{-2} in the summer but were shifted later in the season relative to H. Maximum values of LE were reduced strongly by the first autumn frost on Day 278 (Fig. 4). This inhibition remained even with subsequent mild daytime temperatures and night-time temperatures above freezing.

The distinct annual patterns in H and LE exchange resulted in a large annual variation in energy partitioning at the site. The mid-day (12.00–14.00 hours) Bowen ratio, β (= H/LE), varied from a winter (Dec – Feb) value of 8.7 ± 7.8 to a growing season (May – Sept) value of 1.4 ± 1.6 ($P << 0.01$, $t = 14.3$) (Fig. 5a). The highest β-values in midwinter (Fig. 5b) were associated with extremely cold temperatures at the site and the consequent reduction in the saturation vapour pressure and the potential gradient for driving evaporation or sublimation. The low growing season Bowen ratios indicate that the site was under minimal water stress at this time.

The surface conductance (G_s) at the site was calculated by inverting the Penman–Monteith equation (e.g. Kelliher *et al*. 1992). A plot of mid-day G_s (12.00–14.00 hours on days without precipitation) over the growing season suggests that the increase and decrease in LE observed around days 100 and 280, respectively, are mediated through a change in the bulk surface conductance of the forest (Fig. 6a) which is primarily a function of the amount of leaf area present and stomatal conductance per unit leaf area. After initially increasing in early April (~day 100), the mid-day surface conductance remained at a roughly constant value of ≈4.5 mm s^{-1} for about a month and then increased during June (coincident with new foliage production) to reach a maximum value of ≈7 mm s^{-1} in early July. The mid-day G_s stayed at this value through September and then fell precipitously with the first frosts in October. Surface conductance did not recover to prefrost values even during a stretch of days with warm afternoons and no night frosts (~days 290–300). LAI data from 1998 (Fig. 6a) suggest that the forest leaf area declines by ≈17% in the autumn. The decline in G_s (> 60%), however, is far greater than the change in LAI, suggesting that the physiology of the foliage changed after the frost. Soil temperatures remained above 5 °C up to day 300.

In addition to these seasonal trends, the surface conductance varied as a function of the photosynthetically active photon flux density (PPFD) and the air saturation deficit (D) (Fig. 6b,c). Although the data are highly variable, a best-fit line through the data utilizing the LOWESS technique (Cleveland 1979) suggests that a saturating model describes the relationship between PPFD and G_s. Using the same technique, canopy conductance appears to decline linearly with increasing D, either with or without a threshold of about 1.2 kPa (we cannot assess the significance of the pattern below about 0.5 kPa because it is difficult to accurately measure conductances at low values of D).

Annual pattern of net ecosystem carbon exchange

The forest was a slight source of carbon through the first 90 days of 1996 (Fig. 7), with an average winter respiration rate during this time of ≈0.32 μmol m^{-2}s^{-1}. Day and

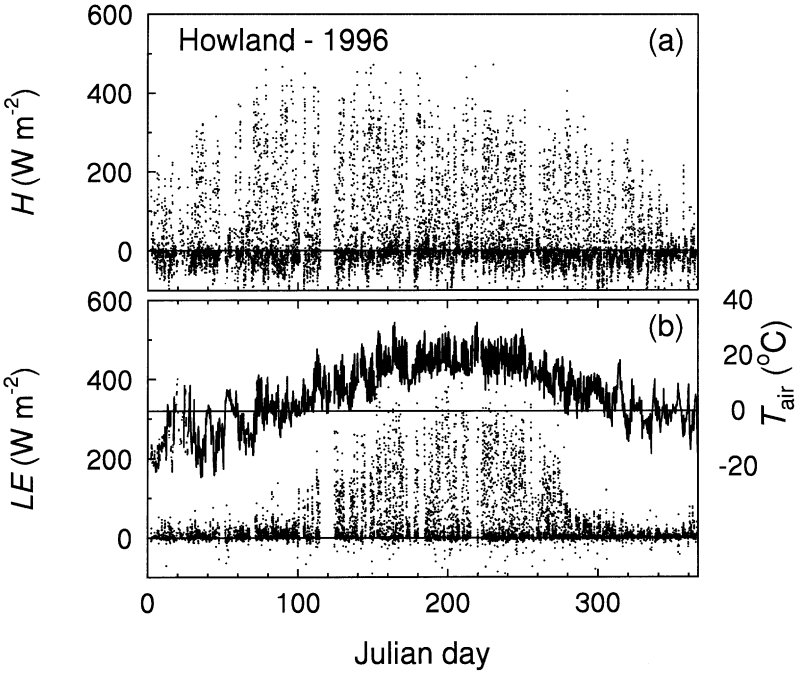

Fig. 4 Annual patterns of (a) sensible and (b) latent heat measured above the Howland forest. Gaps in the record result from instrument failures. The solid line indicates the air temperature measured at 27 m.

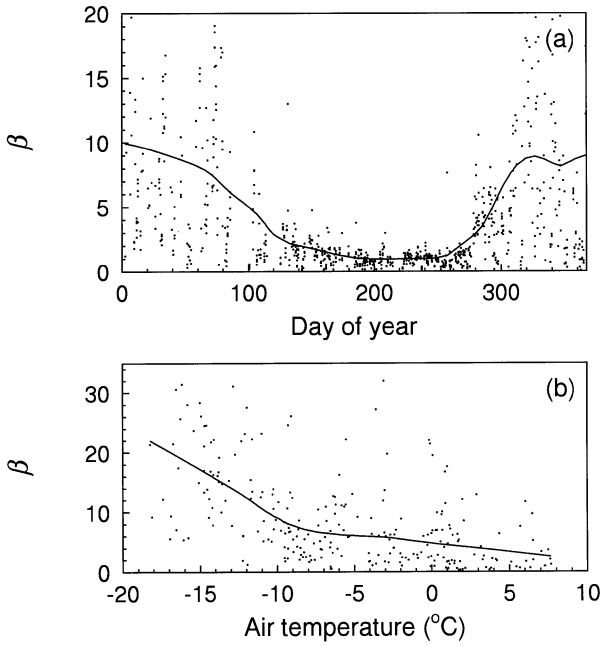

Fig. 5 (a) Mid-day Bowen ratio (β) on dry days. (b) Mid-day Bowen ratio of the Howland forest as a function of air temperature.

night values did not differ significantly when temperatures were below freezing ($P < 0.01$). On sunny winter days when temperatures were above freezing, the forest became a net sink for CO_2 although uptake rates were low, typically $< -2\,\mu mol\,m^{-2}s^{-1}$. With increasing temperatures and the thawing of the soil, net ecosystem exchange increased rapidly from Julian day 95 (Fig. 7). The increase in nocturnal respiration lagged the increase in daytime CO_2 uptake, probably because soil temperature lagged behind air temperature in the early spring.

During the summer (Julian days 173–265), daytime (defined as 30-min time periods with a mean PPFD $> 1\,\mu mol\,m^{-2}s^{-1}$) *NEE* averaged $\approx 6.4\,\mu mol$ CO_2 $m^{-2}s^{-1}$ and nocturnal (defined as 30-min time periods with a mean PPFD $< 1\,\mu mol\,m^{-2}s^{-1}$ and $u^* > 0.15\,m\,s^{-1}$) *NEE* averaged $\approx 6.0\,\mu mol$ CO_2 $m^{-2}s^{-1}$. The mean air temperature during these nocturnal hours was 15.4 °C. Maximum mid-day *NEE* (defined as the 90th-percentile of the *NEE* values between 11.00 and 13.00 hours each day in the summer) was $-19.8\,\mu mol\,m^{-2}s^{-1}$.

Carbon exchange rates were reduced abruptly by the first frost on JD 278 (Fig. 7). CO_2 uptake rates then remained suppressed even after a series of warm days and frost-free nights. Daily photosynthesis continued until a series of days in which maximum temperatures remained below 0 °C, starting on day 320. The abrupt decrease in *NEE* following the first frost of autumn suggests that the timing of this event may be an important regulator of seasonal C exchange in boreal evergreen forests.

Below-canopy carbon exchange

Continuous measurements of the CO_2 flux at 3 m above the ground (F_f) which include understorey and soil

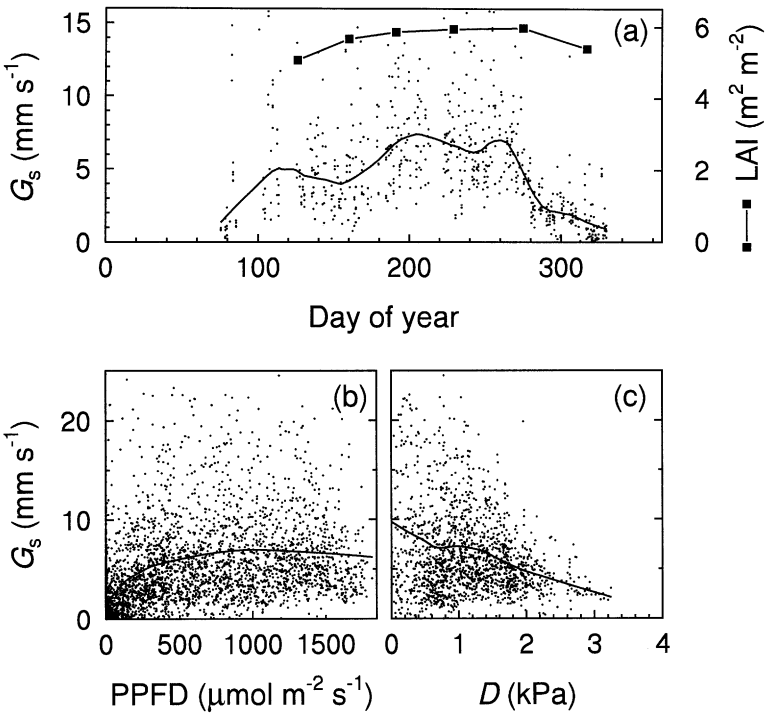

Fig. 6 Canopy conductance (G_s) calculated from the Penman–Monteith equation. (a) Seasonal pattern of mid-day conductance on dry days. Also shown are adjusted LAI measurements made in 1998. (b–c) Relationship between G_s and PPFD, and G_s and saturation deficit (D). Lines indicate smoothed values using the LOWESS technique (Cleveland 1979).

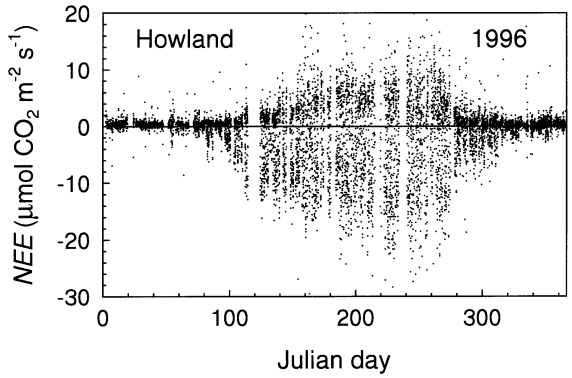

Fig. 7 Annual pattern of net ecosystem CO_2 exchange (NEE) of the Howland forest. Gaps in the record result from instrument failures.

exchanges began in mid-May. The seasonal pattern is characterized by a midsummer maximum of about 2.5 μmol m^{-2}s^{-1} in early August (Julian day 220) and a winter value of about 0.3 μmol m^{-2}s^{-1} reached by late November (Julian day 330) when soil temperatures dropped below 5 °C. The general pattern of CO_2 flux followed that of soil temperature measured at 5-cm depth (Fig. 8a). The below-canopy CO_2 flux represented about 40% of total ecosystem nocturnal respiration in the summer and about 100% of ecosystem respiration by December.

The below-canopy data were quite variable on a 30 minute timescale, even during unstable, mid-day periods. The standard deviation of half-hourly below-canopy CO_2 flux values during the middle of sunny days in July (11.00–13.00 hours, PPFD > 500 μmol m^{-2}s^{-1}) that pass our data acceptance criteria (wind speed > 0.5 m s^{-1}, etc.), for example, was ≈ 60% of the mean. This variation was about three times greater than that of whole ecosystem (NEE) fluxes during the identical time period. We ascribe the greater variance in the understorey data to the more episodic nature of below-canopy exchange, the smaller and more variable below-canopy flux source regions, and the increasing influence of measurement system noise on smaller absolute fluxes. Soil respiration measurements made with chambers (E.A. Davidson, unpubl. data) suggest a somewhat higher rate of below-canopy respiration. We are in the process of resolving the apparent discrepancy between chamber and eddy covariance data.

The net below-canopy CO_2 flux represents the sum of respiration from soil microorganisms, roots, and litter as well as CO_2 uptake by understorey vegetation. Negative values (uptake) were observed rarely indicating that the subcanopy layer acts almost exclusively as a net CO_2 source. Using the whole data set, fair agreement was found between the below-canopy CO_2 flux (F_f) and soil temperature at 5 cm (T_{5cm}) using a Q_{10} model (Fig. 8b):

$$F_f = (F_{ref})(Q_{10})^{(T_{5cm}-T_{ref})/10}, \quad (7)$$

where F_{ref} is the flux at the reference temperature

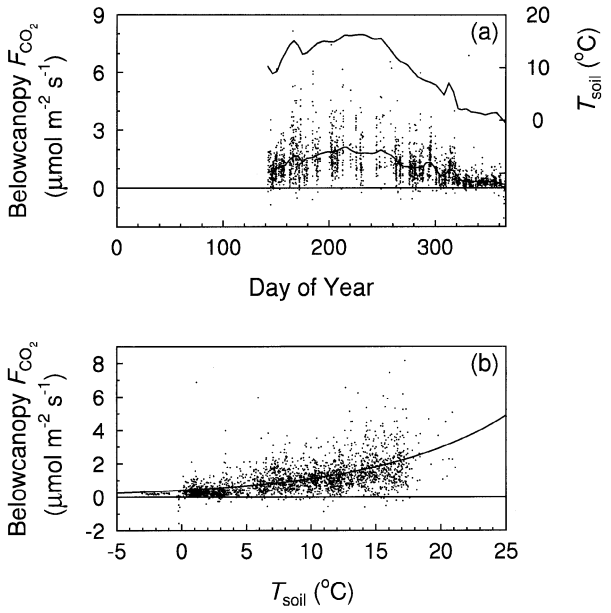

Fig. 8 (a) Annual pattern of forest floor and understorey CO_2 exchange and soil temperature. Understorey measurements began on JD 140. (b) Temperature response of understorey CO_2 exchange. Lines indicate smoothed values using the LOWESS technique.

(= 1.1 μmol m^{-2}s^{-1}), Q_{10} is the temperature coefficient (= 2.7), and T_{ref} is the reference temperature (= 10 °C).

Canopy carbon exchange

Because of the large variance in the 30-min understorey values, canopy CO_2 exchange (F_c) was calculated by subtracting modelled below-canopy CO_2 flux (eqn 7 above) from *NEE*.

The annual CO_2 flux data were divided into 12-time periods for analysis of the relationship between PPFD and canopy CO_2 exchange (Fig. 9). In mid-winter (JD 1–50 and JD 341–366), there was no significant variation in CO_2 exchange with PPFD. This was also true during early and late winter (JD 311–340 and JD 51–100), although some uptake did occur during warmer days at these times of year (Fig. 7). The coefficient of variation (r^2) for simple, rectangular hyperbolae (Michaelis–Menten) models of PPFD and canopy CO_2 exchange (Table 2) were very high during the growing season, ranging from 0.69 to > 0.8. Non-rectangular hyperbolae were not used because the very slight improvement in fit did not warrant the additional degree of freedom. Analysis of residuals suggests that linear models in *D* or 2nd order models in T_{air} accounted for a small (only about 2–27%) but significant amount of the remaining variation in F_c (data not shown).

Fitted coefficients of Michaelis–Menten models of PPFD and canopy CO_2 exchange showed a strong seasonality of response. For example, the seasonal pattern of A_{max}, canopy photosynthetic capacity, shows an increase in capacity of about 0.25 μmol m^{-2}s^{-1} d^{-1} from JD 75 through JD 137, a lower rate of increase through about day 240, and then a sharp drop-off after the first autumn frost (Fig. 10). Similarly, canopy dark respiration (R_d) increases from low early season values to maximum rates coincident with leafout and maximum night-time temperatures in June and also drops sharply in the fall. The fitted values of the half-saturation constant, *K* (PPFD value at which $F_{CO2} = 0.5A_{max}$) increases from low winter values (Fig. 10) but then dips in the early summer before increasing again. Canopy photosynthetic capacity and dark respiration are both significantly correlated with mean daytime temperature (Spearman rank correlation coefficient $r_s = 0.83$ for both; $P < 0.05$, $n = 9$) and A_{max} is also correlated with PPFD level ($r_s = 0.63$, $P < 0.05$, $n = 9$).

Annual carbon balance

Eddy covariance measurements of CO_2 are subject to a variety of errors (Goulden *et al*. 1996b; Moncrieff *et al*. 1996). For long-term measurements, selective-systematic errors (different biases between daytime uptake and nocturnal C loss) are of the greatest concern. We believe that the level topography of our site and our method of correcting the spectral deficiencies of our measurement system reduce any potential selective bias, but this is difficult to address quantitatively.

Values missing from the half-hourly record of annual *NEE* (Fig. 7) were modelled by combining estimates of canopy photosynthesis and understorey respiration. Canopy photosynthesis was modelled with the simple seasonal relationships between PPFD and F_{CO2} (Fig. 9, Table 2) and respiration with (7). If data were missing randomly throughout the record, the average *NEE* of −0.9 μmol m^{-2}s^{-1} would suggest an annual C uptake of about 3.4 t C ha^{-1}. However, missing data are biased toward low uptake (dark, rainy days) and carbon loss time periods (still nights). Using our simple model to estimate missing values, we calculate that the Howland Forest accumulated ≈ 2.1 t C ha^{-1} in 1996. We assign an uncertainty of 25% (0.5 t C ha^{-1}) to this value based on the results of previous studies (e.g. Moncrieff *et al*. 1996).

Discussion

Comparison with other forest ecosystems

Summer evaporation rates and Bowen ratios at the Howland forest were similar to well-watered boreal forests measured elsewhere (e.g. Jarvis *et al*. 1976, 1997).

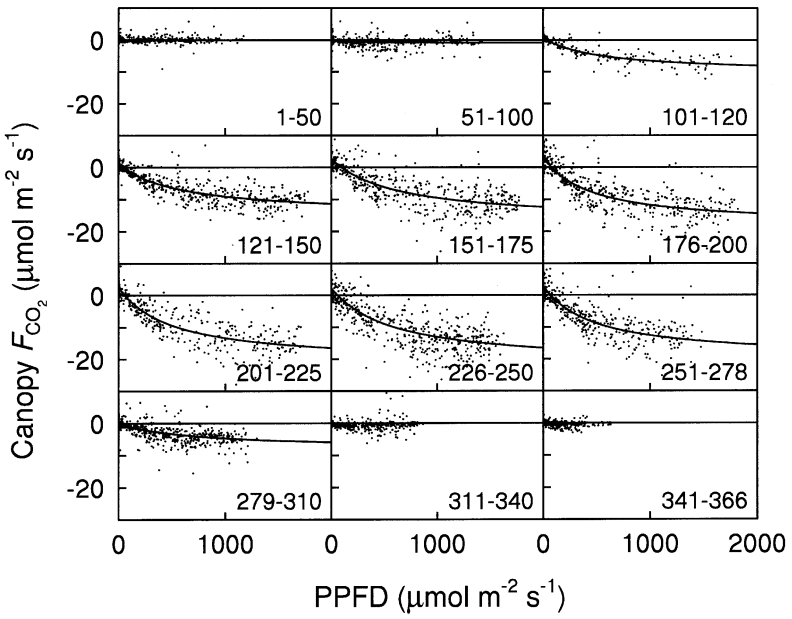

Fig. 9 Seasonal patterns of canopy flux as a function of PPFD.

Table 2 Seasonal variation in coefficients relating canopy CO_2 exchange (F_{CO2}) to PPFD using a rectangular hyperbola (Michaelis–Menten) model: $F_{CO2}=A_{max}I/(K+I)+R_d$, where I is the incident PPFD. (Note that this model is often written as: $F_{CO2}=\alpha A_{max}I/(\alpha I+A_{max})+R_d$ where $\alpha=A_{max}/K$ is the initial slope of the light response curve or canopy photosynthetic efficiency.)

Time period (Day of year)	A_{max} (μmol m^{-2}s^{-1})	K (μmol m^{-2}s^{-1})	R_d (μmol m^{-2}s^{-1})	α	r^2
1–50	–	–	–	–	< 0.01
51–100	−1.1	83	0.11	0.013	0.14
101–120	−11.3	458	0.87	0.025	0.81
121–150	−16.3	463	1.52	0.035	0.84
151–175	−19.9	381	3.88	0.052	0.72
176–200	−22.2	326	4.18	0.068	0.81
201–225	−24.8	386	3.50	0.064	0.85
226–250	−27.6	526	3.42	0.052	0.74
251–278	−25.9	510	3.27	0.051	0.69
279–310	−7.6	392	0.09	0.019	0.50
311–340	–	–	–	–	< 0.01
341–366	–	–	–	–	< 0.01

At the BOREAS southern black-spruce site, β decreased from ≈ 1.9 at the beginning of June to ≈ 1.6 in early July to ≈ 1.3–1.4 from mid-July through mid-September (Jarvis *et al*. 1997), similar to the pattern observed at Howland (Fig. 5a). Over drier boreal larch or pine sites, mid-day, midsummer Bowen ratios were considerably higher, exceeding values of 3 after several days without rain (Kelliher *et al*. 1997; Hollinger *et al*. 1998)

Net mid-day, summer CO_2 uptake (*NEE*) by the Howland spruce–hemlock forest at -12.9 ± 5.9 μmol $m^{-2}s^{-1}$ (mean and standard deviation, $n = 211$) was equivalent to or higher than values from other coniferous, boreal forests. At the northern BOREAS black spruce site (Goulden *et al*. 1997), the mean mid-day summer gross CO_2 uptake rate averaged ≈ –12 μmol $m^{-2}s^{-1}$. CO_2 uptake was ≈ –8 μmol $m^{-2}s^{-1}$ by a black spruce–lichen woodland in Labrador (Fan *et al*. 1995) and a jack pine canopy at the southern BOREAS site (Baldocchi *et al*. 1997), and ≈ –7 μmol $m^{-2}s^{-1}$ at the southern BOREAS black spruce site (Jarvis *et al*. 1997). Over a Siberian larch forest, mid-day uptake rates were still lower at ≈ –4 μmol $m^{-2}s^{-1}$ (Hollinger *et al*. 1998). However, over a boreal aspen forest, mid-day, midsummer uptake rates were higher, reaching ≈ –20 μmol $m^{-2}s^{-1}$ (Black *et al*. 1996).

Carbon uptake saturates at a PPFD of ≈ 500–700 μmol $m^{-2}s^{-1}$ in all of these conifer forests. Although C-uptake declined with increasing saturation deficit in boreal larch forest (Hollinger *et al*. 1998), this response was only weakly observed in the Howland data and not at all in black spruce (Goulden *et al*. 1997).

Midsummer, nocturnal respiration rates at the Howland forest were generally higher than recorded at

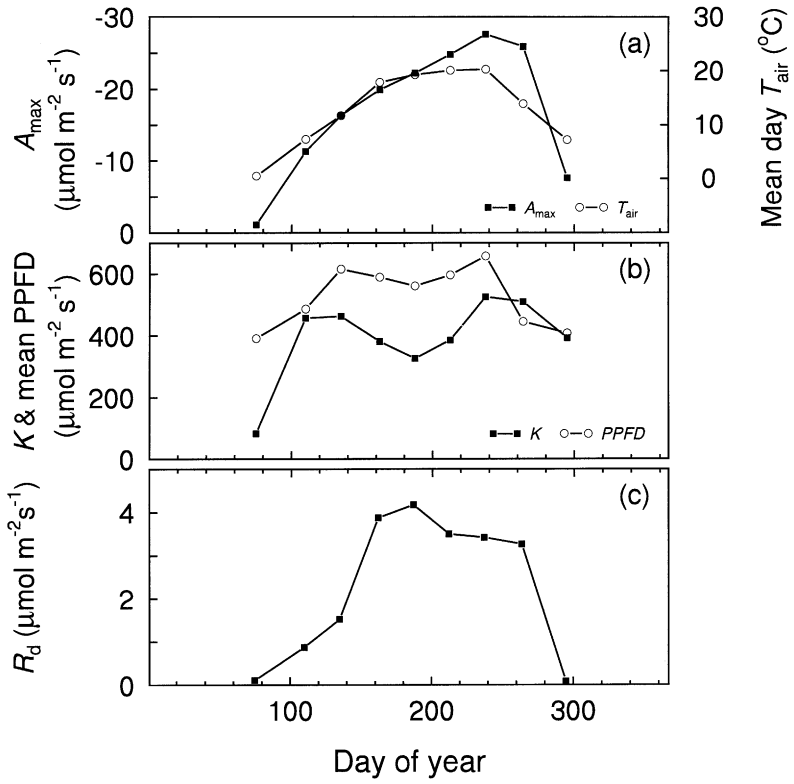

Fig. 10 Seasonal pattern of model coefficients relating canopy CO_2 flux (F_{CO2}) to incident PPFD as $F_{CO2}=A_{max}\cdot I/(K+I)+R_d$, where I is the incident PPFD. (a) Values for A_{max} and mean daytime air temperature. The left *Y*-axis is reversed to better show the correlation between A_{max} and T_{air}. (b) Seasonal pattern of *K* and mean PPFD. (c) Seasonal pattern of inferred canopy respiration.

other coniferous boreal sites. Nocturnal summer *NEE* averaged 6.0 ± 3.4 (n = 349) at a mean air temperature of 15.4 °C. This compares to values of ≈2.5 μmol m^{-2}s^{-1} measured at the BOREAS northern black spruce site (Goulden *et al*. 1997), jack pine site (Baldocchi *et al*. 1997) and Siberian larch (Hollinger *et al*. 1998). Mean nocturnal air temperatures at the Siberian site were similar to those at Howland (≈15 °C) but the BOREAS sites had cooler nocturnal air temperatures (≈10 °C). At an air temperature of 15 °C, we estimate the nocturnal respiration of the BOREAS sites at about 4 μmol m^{-2}s^{-1}.

In contrast to results from previous studies of annual boreal forest C exchange, the coniferous boreal stand at Howland was a strong annual sink for carbon, storing about 2.1 ± 0.5 t C ha^{-1}. Goulden *et al*. (1998) found that the black spruce (*Picea mariana* (Mill.) B.S.P.) stand at the northern BOREAS site (55.879°N, 98.484°W) lost 0.7 ± 0.5 t C ha^{-1} from October 1994 to October 1995 and 0.2 ± 0.5 t C ha^{-1} in the same time period in 1995–96. However, the site was a sink for 0.1 ± 0.5 t C ha^{-1} from October 1996 to October 1997. These authors found that an average uptake over the three years of about 0.6 t C ha^{-1} y^{-1} in woody biomass and moss was more than offset by losses from the soil carbon pool. They ascribed this result to a recent increase in the depth of the soil active layer brought on by warmer temperatures. The BOREAS result was echoed in a study of Scots pine (*Pinus sylvestris* L.) and Norway spruce (*Picea abies* (L.) Karst.) stands growing in central Sweden (60.08°N, 17.48°E) (Lindroth *et al*. 1998). Although the trees in the Swedish study were gaining biomass, the site lost 0.9 t C ha^{-1} between 1 June 1994 and 31 May 1995, and 0.6 t C ha^{-1} over the equivalent period in the next year. Recent climatic changes may have favoured soil respiration over above-ground production in this forest, although management practices (drainage ditches) probably also contributed to enhanced respiration by reducing soil anoxia (Gorham 1995; Lindroth *et al*. 1998).

The net annual C uptake in the Howland forest is comparable to the long-term average at the more southerly deciduous Harvard Forest site (Goulden *et al*. 1996a). Although maximum rates of uptake are greater at the Harvard forest than at Howland, the longer growing season in the evergreen forest at Howland compensates with the result that both sites have similar annual rates of C storage.

Impact of frosts

One of the most significant findings from this study is the apparent importance of temperature thresholds for the regulation of ecosystem CO_2 exchange. Two thresholds, both concerned with the zero °C isotherm were identified and appear to affect physiology at least in part via an effect on stomatal conductance. The first threshold appears to be the spring thawing of forest soils. Prior

to this time the estimated canopy conductance is severely constrained (Fig. 6a). We can assume that the mechanism responsible is the lack of flow of water through the soil and into the trees. The second threshold appears to be the first autumnal frost $<\approx -1$ °C. A reduction in conifer photosynthesis following nights with subfreezing temperatures is well known (e.g. Delucia & Smith 1987; Hällgren *et al*. 1990) but the effect of this event on seasonal CO_2 exchange is striking (Fig. 7).

Springtime thaw and autumnal frosts can occur over large regions in a short period of time since they are often brought about by synoptic events. These may take the form of warm fronts (with or without precipitation) in the spring, and large high pressure events (cold fronts) in the autumn. The result of these synoptic events is that the CO_2 exchange of thousands of square kilometres of landscape may be switched on or off almost simultaneously. The timing of the spring thaw and first major frost varies between years. The date of the spring thaw is less precise than the first frost because snow and ice-melt beneath a canopy is typically patchy. The date of last snow melt at Howland has varied by 10 days over the 1990–98 period. The date of the first −1 °C autumn frost at Howland has been more variable, ranging between day 263 and 294 over the 1987–97 period (day 278.7 ± 8.7, mean and standard deviation). The difference of 31 days between the earliest and latest frosts represents an increase of almost 20% in season length. There is evidence that the length of the northern hemisphere growing season may be increasing and that this may affect C sequestration over large areas (Myneni *et al*. 1997; Randerson *et al*. 1997). Our results point to mechanisms for initiating or concluding seasonal C gain in coniferous, boreal forests.

There are good prospects for being able to remotely monitor the freeze–thaw status of large areas of vegetation and soils via synthetic aperture radar (Way *et al*. 1997). The dielectric constant of water decreases abruptly with freezing and this results in a decrease in radar backscatter. This remotely sensed phenomenon may find utility as a 'switch' for turning on and off carbon exchange (or water stress) in large-scale models of vegetation function.

Conclusions

In addition to the importance of freezing temperatures, our results suggest that boreal C exchange models must account for the large seasonal variation in the rate of maximum canopy photosynthetic capacity (A_{max}). In many models A_{max} is a function of LAI or canopy nitrogen, but these characteristics of the Howland canopy change only slightly over a season (e.g. Figure 6a, D.Y. Hollinger unpubl. data). The correlation of A_{max} with mean daytime temperature suggests that a potential mechanism for such seasonal variation is the acclimation of leaf-level photosynthesis to growth temperature along with a general increase in the absolute value of photosynthesis with temperature (Woodward & Smith 1994). For these reasons we hypothesize that a correlation between mean daytime temperature and A_{max} will be found within and between other vegetation types as well.

The responses of ecosystem CO_2, heat, and water vapour exchange to light, temperature, and other environmental factors in *Picea rubens* forest are remarkably similar to those observed in *Picea mariana* (Goulden *et al*. 1997; Jarvis *et al*. 1997). Functional similarities between the spruce stands include the low growing season Bowen ratio, the early peak and then decrease in H as the forest becomes active, the seasonal increase in photosynthesis before respiration, and the effect of frosts on forest metabolism. The convergence of response between spruce species provides strong support for the concept of functional types. A key goal for future flux studies should be the identification and classification of such types.

Acknowledgements

We thank International Paper and International Paper Timberlands Operating Company, Ltd. for providing access to the Northern Experiment Forest Atmospheric Effects research site in Howland, Maine. Thanks also to Steve Frolking for pointing out the ability of SAR to identify frozen terrain and to Mike Goulden and an anonymous reviewer for their suggestions which improved the manuscript. This research was supported through the NSF/DOE/NASA/USDA Interagency Program on Terrestrial Ecology and Global Change (TECO) by the NSF Division of Environmental Biology under grant number DEB-9524069, by the National Institute for Global Environmental Change (NIGEC) Northeastern Region, and by the USDA Forest Service Northern Global Change Program.

References

Baldocchi DD, Hicks BB, Myers TP (1988) Measuring biosphere-atmosphere exchanges of biologically related gases with micrometeorological methods. *Ecology*, **69,** 1331–1340.

Baldocchi DD, Vogel C (1996) A comparative study of water vapor, energy, and CO2 flux densities above and below a temperate broadleaf and boreal pine forest. *Tree Physiology*, **16,** 5–16.

Baldocchi DD, Vogel CA, Hall B (1997) Seasonal variation of carbon dioxide exchange rates above and below a boreal jack pine forest. *Agricultural and Forest Meteorology*, **83,** 147–170.

Bender M, Ellis T, Tans P, Francey R, Lowe D (1996) Variability in the O_2/N_2 ratio of southern hemisphere air. 1991–94: Implications for the carbon cycle. *Global Biogeochemical Cycles*, **10,** 9–21.

Black TA, den Hartog G, Neumann HH *et al.* (1996) Annual cycles of water vapour and carbon dioxide fluxes in and above a boreal aspen forest. *Global Change Biology*, **2,** 219–230.

Ciais P, Tans PP, White JW *et al.* (1995) Partitioning of ocean and land uptake of CO_2 as inferred by $\delta^{13}C$ measurements from the NOAA/CMDL global air sampling network. *Journal of Geophysical Research*, **100,** 5051–5070.

Cleveland WS (1979) Robust locally weighted regression and smoothing scatterplots. *Journal of the American Statistical Association*, **74,** 829–836.

Conway TJ, Tans PP, Waterman LS, Thoning KW, Kitzis DR, Masarie KA, Zhang N (1994) Evidence for interannual variability of the carbon cycle from the National Oceanic and Atmospheric Administration/Climate Monitoring and Diagnostic Laboratory global air sampling network. *Journal of Geophysical Research*, **99,** 22831–22855.

Delucia EH, Smith WK (1987) Air and soil temperature limitations on photosynthesis in Englemann spruce during summer. *Canadian Journal of Forest Research*, **17,** 527–533.

Fan S-M, Goulden ML, Munger JW *et al.* (1995) Environmental controls on the photosynthesis and respiration of a boreal lichen woodland: a growing season of whole-ecosystem exchange measurements by eddy correlation. *Oecologia*, **102,** 443–452.

Fassnacht KS, Gower ST, Norman JM, McMurtrie RE (1994) A comparison of optical and direct methods for estimating foliage surface area index in forests. *Agricultural and Forest Meteorology*, **71,** 183–207.

Fernandez IJ, Rustad LE, Lawrence GB (1993) Estimating total soil mass, nutrient content, and trace metals in soils under a low elevation spruce-fir forest. *Canadian Journal of Soil Science*, **73,** 317–328.

Gorham E (1995) The Biogeochemistry of Northern Peatlands and Its Possible Responses to Global Warming. In: *Biotic Feedbacks in the Global Climatic System: Will the Warning Feed the Warming?* (eds Woodwell GM, Mackenzie F), pp. 169–187. Oxford University Press, New York.

Goulden ML, Daube BC, Fan S-M, Sutton DJ, Bazzaz A, Munger JW, Wofsy SC (1997) Physiological responses of black spruce forest to weather. *Journal of Geophysical Research*, **102,** 28987–28996.

Goulden ML, Munger JW, Fan S-M, Daube BC, Wofsy SC (1996a) CO_2 exchange by a deciduous forest: response to interannual climate variability. *Science*, **271,** 1576–1578.

Goulden ML, Munger JW, Fan S-M, Daube BC, Wofsy SC (1996b) Measurements of carbon sequestration by long-term eddy covariance: Methods and a critical evaluation of accuracy. *Global Change Biology*, **2,** 169–182.

Goulden ML, Wofsy SC, Harden JW *et al.* (1998) Sensitivity of boreal forest carbon balance to soil thaw. *Science*, **279,** 214–217.

Hällgren J, Lundmark-ET, Strand M (1990) Photosynthesis of Scots pine in the field after night frosts during summer. *Plant Physiology and Biochemistry*, **28,** 437–445.

Hollinger DY, Kelliher FM, Schulze E-D *et al.* (1998) Forest-atmosphere carbon dioxide exchange in eastern Siberia. *Agricultural and Forest Meteorology*, **90,** 291–306.

Hollinger DY, Kelliher FM, Schulze E-D *et al.* (1995) Initial assessment of multi-scale measures of CO_2 and H_2O flux in the Siberian taiga. *Journal of Biogeography*, **22,** 425–431.

Jarvis PG, James GB, Landsberg JJ (1976) Coniferous forest. In: *Vegetation and the Atmosphere* (ed. Monteith JL), pp. 171–240. Academic Press, San Diego, CA.

Jarvis PG, Massheder JM, Hale SE, Moncrieff JB, Rayment M, Scott SL (1997) Seasonal variation of carbon dioxide, water vapor, and energy exchanges of a boreal black spruce forest. *Journal of Geophysical Research*, **102,** 28953–28966.

Kaimal JC, Gaynor JE (1991) Another look at sonic thermometry. *Boundary-Layer Meteorology*, **56,** 401–410.

Keeling RF, Piper SC, Heimann M (1996) Global and hemispheric CO_2 sinks deduced from changes in atmospheric O_2 concentration. *Nature*, **381,** 218–221.

Kelliher FM, Hollinger DY, Schulze E-D *et al.* (1997) Evaporation from an Eastern Siberian larch forest. *Agricultural and Forest Meteorology*, **85,** 135–147.

Kelliher FM, Köstner BM, Hollinger DY *et al.* (1992) Evaporation, xylem sap flow, and tree transpiration in a New Zealand broad-leaved forest. *Agricultural and Forest Meteorology*, **62,** 53–73.

Lindroth A, Grelle A, Morén A-S (1998) Long-term measurements of boreal forest carbon balance reveal large temperature sensitivity. *Global Change Biology*, **4,** 443–450.

McMillen RT (1988) An eddy correlation technique with extended applicability to non-simple terrain. *Boundary-Layer Meteorology*, **43,** 231–245.

Moncrieff JB, Malhi Y, Leuning R (1996) The propagation of errors in long-term measurements of land atmosphere fluxes of carbon and water. *Global Change Biology*, **3,** 231–240.

Moore CJ (1986) Frequency response corrections for eddy correlation systems. *Boundary-Layer Meteorology*, **37,** 17–35.

Myneni RB, Keeling CD, Tucker CJ, Asrar G, Nemani RR (1997) Increased plant growth in the northern high latitudes from 1981 to 1991. *Nature*, **386,** 698–702.

Randerson JT, Thompson MV, Conway TJ, Fung IY, Field CB (1997) The contribution of terrestrial sources and sinks to trends in the seasonal cycle of atmospheric carbon dioxide. *Global Biogeochemical Cycles*, **11,** 535–560.

Stenberg P (1996) Correcting LAI-2000 estimates for the clumping of needles in shoots of conifers. *Agricultural and Forest Meteorology*, **79,** 1–8.

Tans PP, Fung IY, Takahashi T (1990) Observational constraints on the global atmospheric CO_2 budget. *Science*, **247,** 1431–1438.

Vose RS, Schmoyer RL, Steurer PM, Peterson TC, Heim R, Karl TR, Eischeid JK (1992) The global historical climatology network: Long-term monthly temperature, precipitation, sea level pressure, and station pressure data. *ORNL/CDIAC-53, NDP-041.* Carbon Dioxide Information and Analysis Center, Oak Ridge National Laboratory, Oak Ridge, Tennessee, USA.

Way J, Zimmermann R, Rignot E, McDonald K, Oren R (1997) Winter and spring thaw as observed with imaging radar at BOREAS. *Journal of Geophysical Research*, **102,** 29673–29684.

Webb EK, Pearman GI, Leuning R (1980) Correction of flux measurements for density effects due to heat and water vapor transfer. *Quarterly Journal of the Royal Meteorological Society*, **106,** 85–100.

Woodward FI, Smith TM (1994) Global Photosynthesis and Stomatal Conductance: Modeling the Controls by Soil and Climate. *Advances in Botanical Research*, **20,** 2–41.